This project is funded by the European Union

AHEAD Workpackage 8
JRA X-ray Optics

Deliverable D8.11 - D45

Report on the performance verification of the collimated X-ray beam for the testing of high resolution optics

Written by	Carlo Pelliciari (MPE)	
Checked by	Vadim Burwitz (MPE)	
Distribution List	AHEAD Management Team Vadim Burwitz (MPE) Dick Willingale (ULeic) René Hudec (CTU) Gianpiero Tagliaferri (INAF/OAB)	
Distribution Date	Draft Version Final Version	Dec 26, 2018 Feb 27, 2019

Acronym list

ATHENA Advanced Telescope for High Energy Astrophysics
MM Mirror Module
SPO Silicon Pores Optics
eROSITA extended ROentgen Survey with an Imaging Telescope Array
HEW Half Energy Width
PANTER PAntolsky Neuried TEstanlage Röntgen
PIXI Princeton Instruments X-ray Imager
PSF Point Spread Function
TRoPIC Third Roentgen Photon Imaging Camera
ZP Zone Plate
ZPC Zone Plate Collimator
eROqm eROSITA qualification model

Contents

This project is funded by the European Union

Abstract

At the PAntolsky Neuried TEstanlage Röntgen (PANTER) X-ray test facility Zone Plate Collimators (ZPCs) have been designed, constructed and measured [1] [2] [3]. The results show they can produce a parallel beam with a divergence smaller than one arc-second. In this document we report the characterization of optics with different focal lengths using the beam generated by a ZPC.
A parallel beam provides three main contributions to the final image:

- a smaller PSF because the source is as like a point source at infinity,
- a larger effective area because a parallel beam illuminates the entire surface of the mirrors,
- formation of the image at the real focal length of the optics.

At present time, the contribution of the ZPC is not appreciable in term of Point Spread Function (PSF) resolution because the PSF of the tested optics is bigger than the X-ray source spot. As a consequence, the dimension of the focal spot measured with and without ZPC are similar. On the contrary, the test campaigns illustrate that with the ZPC the image is focused at a shorter distance compared to the image distance obtained with a divergent beam (thin lens equation).
These tests are sufficient to confirm that the setup implemented at the PANTER facility can be used is to characterize the master Mirror Module (MM) necessary for the validation of the Beatrix facility [4] [5].

1 Introduction

The Zone Plate (ZP) has been designed [1] to diffract an X-ray beam with the energy corresponding the fluorescence line of Al-k (~1.5 keV). The ZPC produces a beam with a divergence ($\ll$ 1 arcsec) much smaller than the master MM that has to be tested and validated ($\simeq$ 5 arcsec).
The beam produced at the PANTER X-ray facility has two divergence components: one is due to the fact that the source has a finite dimension, the other is due to the fact that the beam is emitted on a hemisphere.
The X-ray beam of the PANTER facility is generated by a bremsstrahlung source with a estimated diameter size of $\simeq$ 0.3 mm [6]. Every point of the source emits in any direction inside of a solid angle of 2π sr. The source is located at approximately 123 meters from the optics and it emits in a hemisphere with a small angular distribution gradient. The beam has a divergence of 0.5 degree on the full tube aperture. In this range the gradient of the angular photon distribution is not measurable. In other words is negligible for our application. The beam shows a component of divergence due to the source point like shape that generate a spherical wave overlapped to a broadening component due to the finite dimension of the source itself. Divergence and broadening of the source respectively increase the distance were the image is focused and the dimension of the spot itself compared to the theoretical one. However, it is not possible to appreciate the contribution of the finite size of the source to the PSF because the contribution to divergence due to the optics is much higher. Therefore, the distance of the image formation from the optics, is the parameter that show the biggest variation due to the introduction of the ZPC.

1.1 Experimental setup available at the PANTER facility with and without ZP

In this section we summarize the setups available to characterize optics with different radii of curvatures and focal lengths:

- Setup with optics and detector in the big chamber (section 1.1.1).
- Setup with optics in the big chamber and detector extension chamber: this is used for focal lengths that are bigger than 12 meters. The setup was designed for 20 meters focal length optics and with reflection angle of about 2.7 degree.(section 1.1.2)
- Setup with optics in the tube that connect the chamber to the X-ray source. Optics are mounted at the end of the 1 meter tube, just a couple of meters before the big chamber. This setup is used for optics with a focal length between 10 and 12 meters.

1.1.1 Setup for short focal length optics, i.e smaller than 9 meters

If the focal length is shorter than 9 meters it is possible to mount the optics directly in the big chamber. This configuration has been used to characterize the mirror modules of extended ROentgen Survey with an Imaging Telescope Array (eROSITA) with a focal length of 1.6 meters.
The eROSITA mirror module has been tested with and without ZPC. The setup is reported in figure 1. Details of mask, mirror module and ZPC are visible respectively in figures 2(a) and 2(b). The comparison of the measurement with and without ZPC are reported in section 3, figure 21.

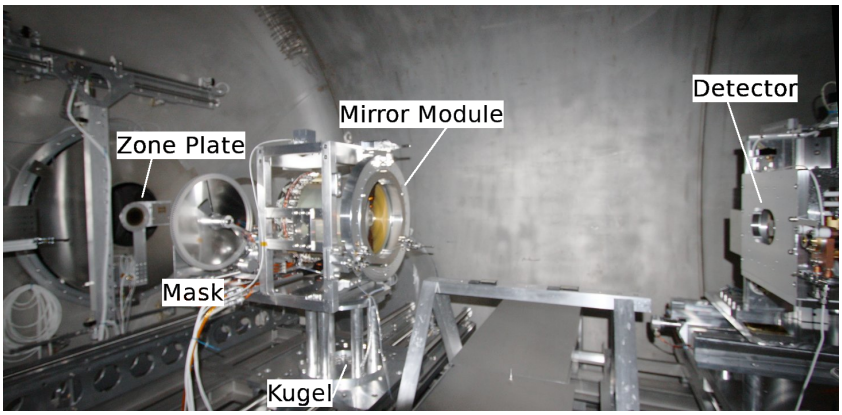

Figure 1: Setup for the short focal length. All component are mounted in the big vacuum chamber. From the left: ZP, mask for mirror module sector analysis, mirror module, detectors. The focal lengh is 1.6 meters.

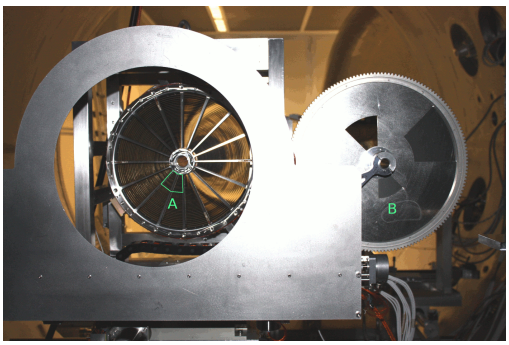

(a) Left: eROSITA mirror module. Right: the mask.

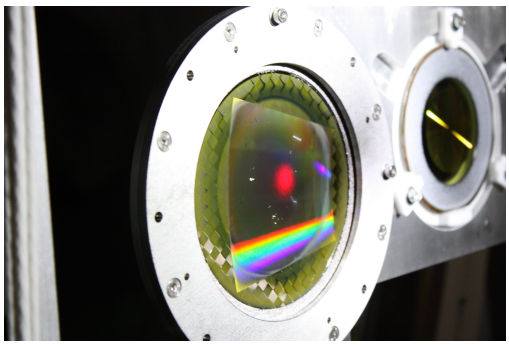

(b) The 6 inch ZP

Figure 2: Setup for the characterization of the eROSITA mirror module with the 6 inch ZP.

1.1.2 Setup for 20 meters focal length optics

The chamber extension has been designed [7] for optics with about 20 meters focal length. Because the PANTER X-ray source is a finite distance and it is divergent, the image is expected to be at about 24 meters[1] from the optics.
Figure 3(a) illustrates a view from side of the tank-e. the tank-e (chamber extension) is 3 meter long with a diameter of 0.8 m. It can be positioned at different distance from the big chamber. A modular vacuum tube with a diameter of 250 mm is connected between big chamber and tank-e. Inside of the chamber, the detector Princeton Instruments X-ray Imager (PIXI) can be moved in a range of 2 meters along the X-ray beam and in the focal plane with a three axis system.

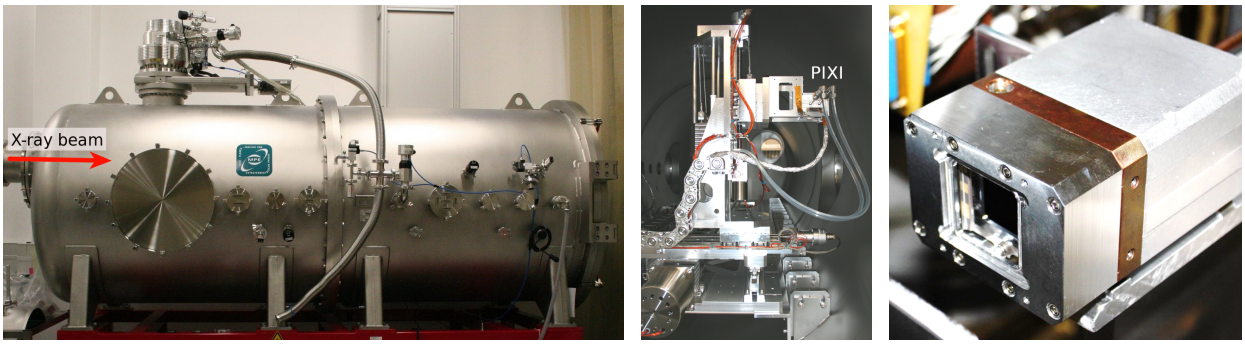

(a) View from side of the extension chamber (Tank-e) (b) Inside Tank-e. (c) Detector PIXI.

Figure 3: From top-left: extension chamber and detector.

The tube is designed to have an angle of 2.7 degrees with respect to the PANTER optical axis. Small angle tuning of ± 0.2 degrees are possible. The Optics is mounted on the Kugel position (Figure 5(b) and the reflection is detected 24 meters far in the tank-e. In the tank-e can fit only the PIXI detector (Figure 3(c)). This setup (Sketch in figure 4) has been used to demonstrate that is possible to separate the image created by the beams of different order diffracted from the ZPC. These results are reported in section 2.1.

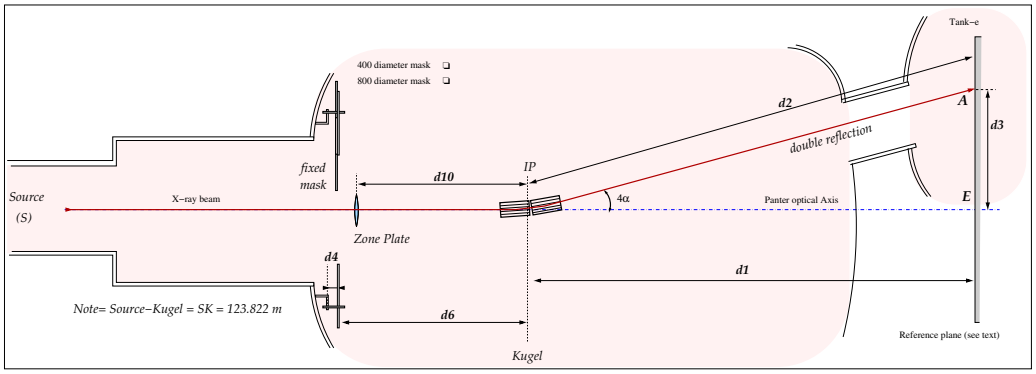

Figure 4: Setup of ZP with a 20 meters focal length optics and at an image distance of about 24 meter. The MM is in the big chamber and the detector is in the extension (i.e. reference plane).

[1]The result is obtained using the thin lens equation with a source distance of 123 meters, rounding to the meter.

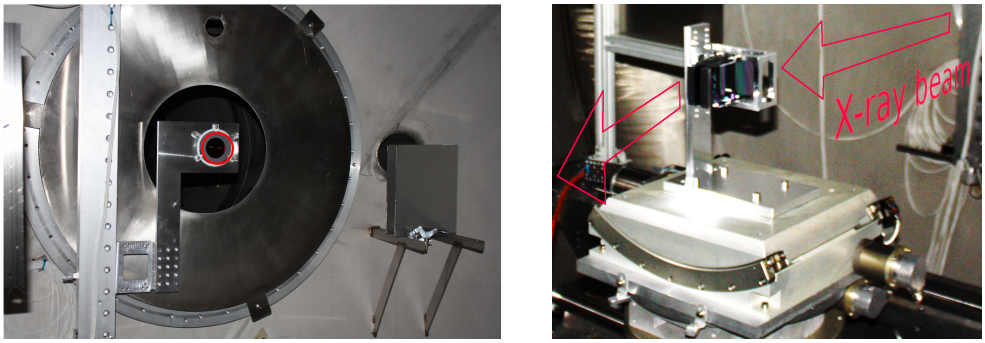

(a) Zone Plate (b) Mirror module

Figure 5: Zone plate and mirror module respectively mounted at the end of the 120 meters tube and on the Kugel.

1.1.3 Setup for 12 meters focal length optics

For completeness, in this section we describe the PANTER setups to characterize optics with focal length between 8.5 and 12 meters.

1. Setup without ZPC. The MM is in the tube and the detector is in the chamber. Figure 6
2. Setup without ZPC. The MM is in the chamber and the detector is the extension chamber. Figure 7
3. Setup with ZPC. ZPC, optics and detector in the big chamber. The setup is under implementation. Sketch reported in figure 8. This setup will be used to characterize the master XOU for the BEATRIX validation.

The setups described at points 1 and 2 have been extensively used to characterize several MMs [6] [7].

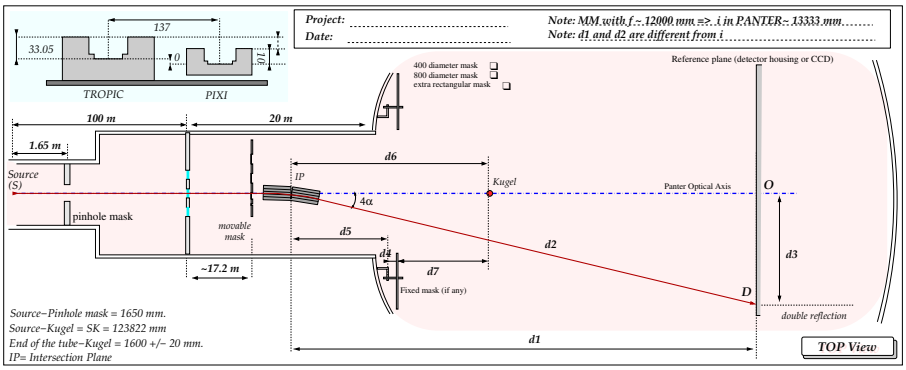

Figure 6: Setup without ZPC. The MM is in the tube and the detector is in the chamber.

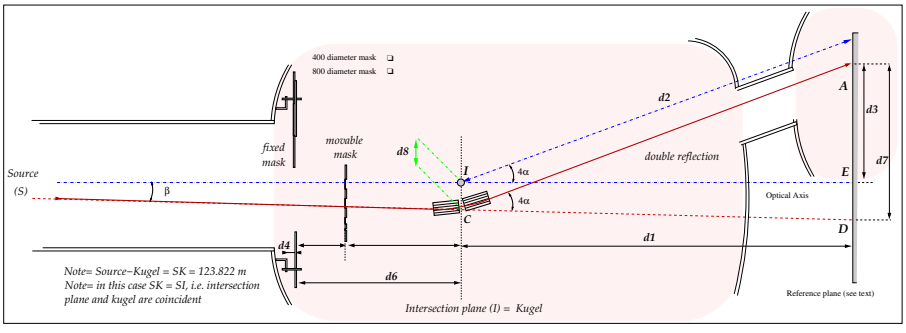

Figure 7: Setup without zone plate. The MM is in the chamber and the detector is the extension chamber.

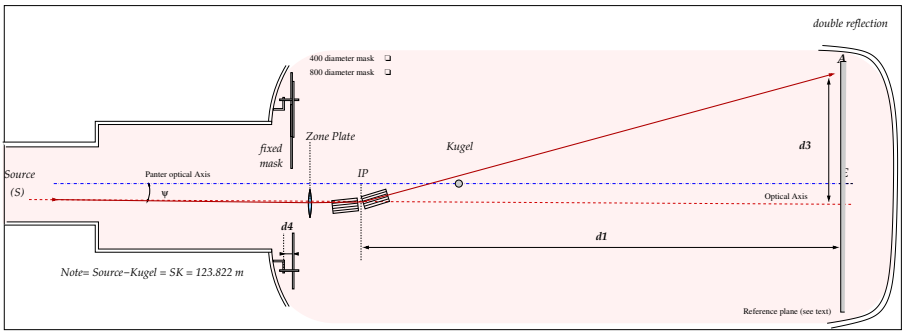

Figure 8: The big chamber is 12.850 meters long. The ZPC and the optics has to be mounted respectively 200 and 400 mm from the begin of the chamber. In the same time, the detector support has to be modified to be able to operate at the limits of the chamber itself. This setup will be used to characterize the master XOU for the BEATRIX validation.

This project is funded by the European Union

2 X-ray performances of the ZPC

In this section we report the diffraction efficiency and the angular resolution of the ZPC. The setup has been already described [2]. The sketch of the setup is also reported in picture 9. Direct and diffracted beam pass trough the pin-holes of the multi-pin-hole mask. Direct beam and diffracted beams creates multiple spot images. The images with higher intensity are given for direct beam and m=+1 and m=-1 orders. The image of diffracted (m=+1 and m=-1 orders) and direct beam are analyzed as reported in figure 10: a automated software recognize the brightest spot and calculate:

- the α_{col}, i.e. the angle between the direct and collimated beam for every ;
- the α_{div}, i.e. the divergence of the beam for each pin-hole of the mask;
- the difference $\Delta\alpha = \alpha_{col} - \alpha_{div}$. This difference, theoretically should be zero. In practice each point is affected by statistical errors due to the count rate, the error in shape of the pin-hole (mechanical error), the aberration introduced by the ZPC. All this physical quantity affect the value and the direction of $\Delta\alpha$. The Value give information about the maximum error in resolution. A trend in the direction gives information about possible aberration.

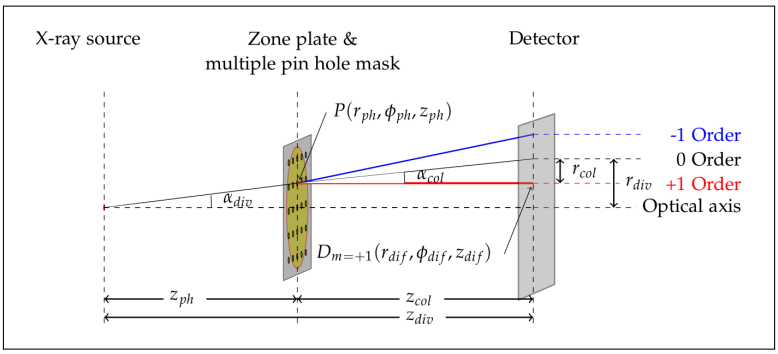

Figure 9: Schematic of the experimental setup: X-ray source, ZP, multiple pin hole mask and detector. The diffracted wave front through the pin hole at position $P(r_{ph}, \phi_{ph}, z_{ph})$ yields a tuple of rays at positions $D_m(r_{dif}, \phi_{dif}, z_{dif})$ in the detector plane. In the collimator configuration, the rays of diffraction order m = +1 are parallel to the optical axis (dashed line).

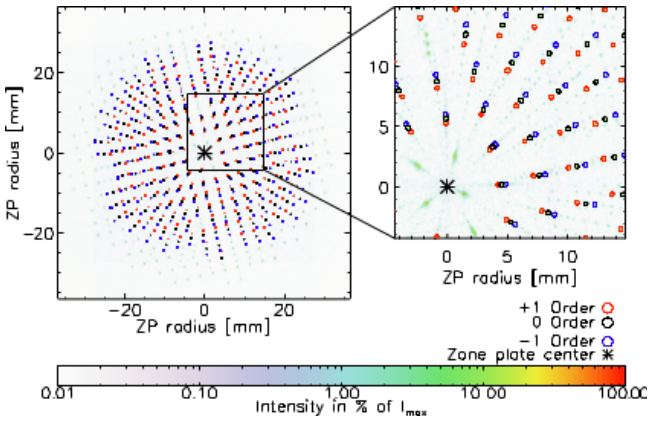

Figure 10: A representative measurement (12h integration time) employing the experimental set-up shown in Fig. 9. For each pin hole a tuple of spots is measured in the detector plane. The resulting source detections position are over-plotted with circles. The corresponding diffraction orders are color coded: the collimated +1 order (red), the not diffracted direct 0 order (black), and the divergent -1 order (blue). The faint spots that are not fitted are due to the contribution from higher diffraction orders.

2.1 Characterization of the 4 inch ZPC

In this section we report the angular resolution and diffraction efficiency for the 4 inch ZPC (Fig. 11).

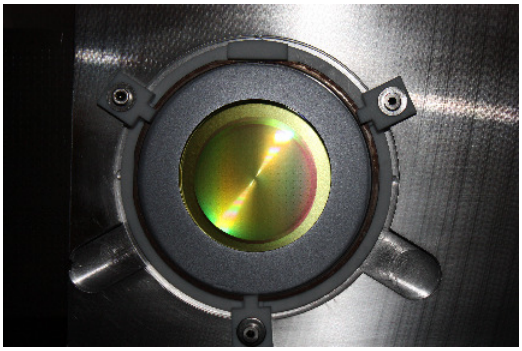

Figure 11: Phase zone plate optimized for an energy of the Al-K$_\alpha$ emission line at 1.49 keV mounted in the PANTER X-ray test facility. Trenches with a depth of 2.35 µm are etched into a thin polyimide film (10 µm thick) which has been structured via e-beam lithography. The structured area, with a diameter of 5 cm, provides a geometrical area of 20 cm^2.

2.1.1 Angular resolution

The results obtained for the angular resolution are shown in Fig. 12. The intensity image, using basically the same data as shown in Fig. 10, is analyzed in order to determine values for the angular resolution.
The top panel of Fig. 12 shows the measured divergence angle α_{div} and the measured collimation angle α_{col} depending on the ZP radius. The measured angles are in agreement with the divergence of a source at a distance of 131.8 m, which is over-plotted with the dashed blue line.
The second and third panel show the collimation quality measured by the difference of $\alpha_{col} - \alpha_{div}$ depending on radius and azimuth, respectively. Both plots show no significant trend within the errors of 0.1 arc sec. On average, the values of $\alpha_{col} - \alpha_{div}$ are (0.03 ± 0.13) arc sec.

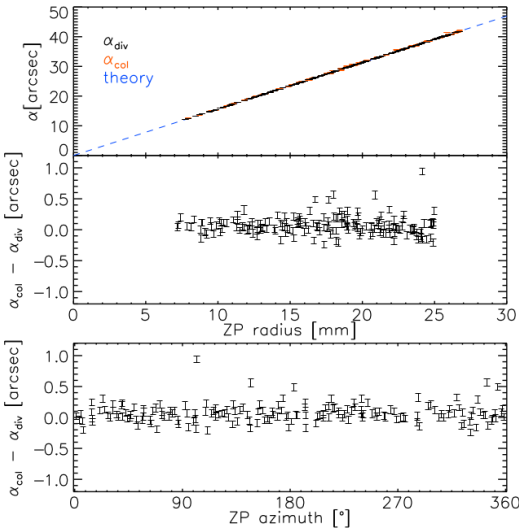

Figure 12: Results obtained for the angular resolution of the ZPC. The top panel shows the measured divergence angle α_{div} and the measured collimation angle α_{col} depending on the ZP radius. The measured angles are in agreement with the divergence of a source at a distance of 131.8 m, which is over-plotted with the dashed blue line. The second and third panel show the collimation quality measured by the difference of $\alpha_{col} - \alpha_{div}$ depending on radius and azimuth respectively.

Summarizing the results obtained for the angular resolution, a ZP can be used as collimator for the PANTER X-ray test facility. The measurements presented here provide an upper limit for the aberrations in angular resolution of 0.13 arc sec. It can be concluded that the alignment of the individual components, and especially of the ZP, is adequate for the proposed collimator. Also the resolution of the individual components, i.e. the

resolution of the source, the ZP, and the detector, do not significantly influence the results. For the planned application, to investigate Advanced Telescope for High Energy Astrophysics (ATHENA) type optics with a resolution of 5 arc sec the *4 inch design* ZP provides sufficient accuracy in angular resolution.

2.1.2 Efficiency

The measured diffraction efficiencies are shown for order $m = 1$ and $m = 0$, the collimated and the direct beam respectively, in Fig. 13. The results are obtained from the same measurements that are used to determine the angular resolution in Sect. 2.1.1. A reference measurement (I^0) without ZP has been used to calculate the diffraction efficiency.

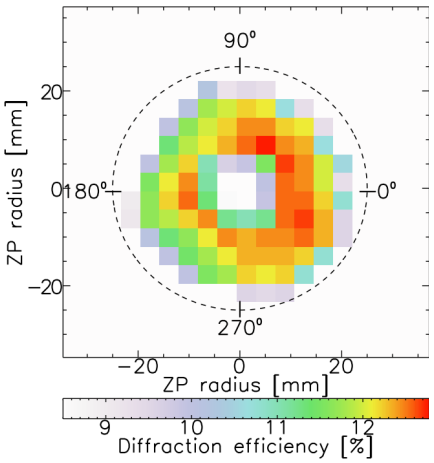

(a) Diffraction order m = +1: Two-dimensional map.

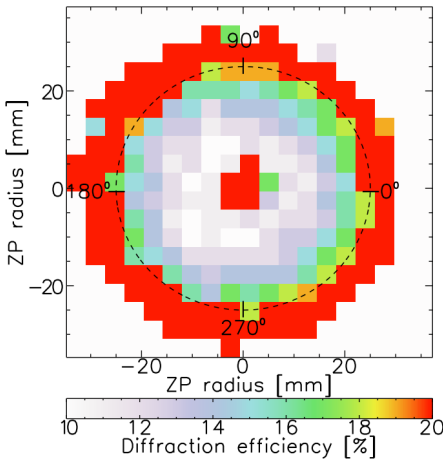

(b) Diffraction order $m = 0$: Two-dimensional map.

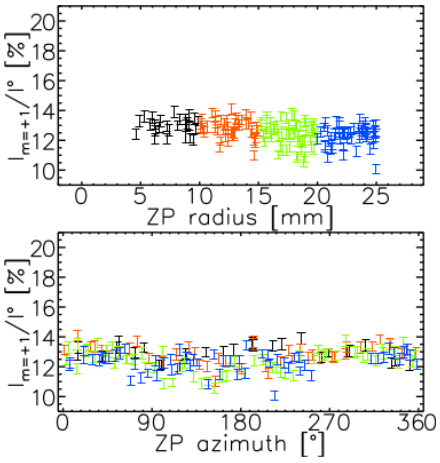

(c) Diffraction order m = +1: Radial (top) and azimuthal (bottom) dependent diffraction efficiency.

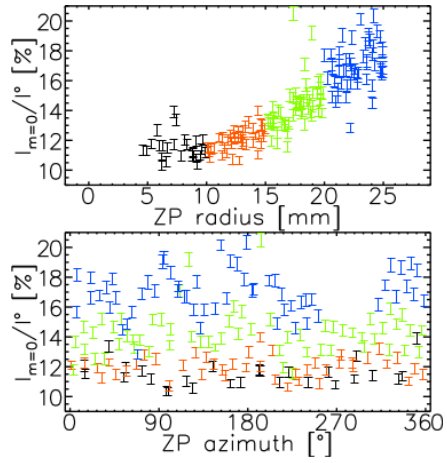

(d) Diffraction order $m = 0$: Radial (top) and azimuthal (bottom) dependent diffraction efficiency.

Figure 13: The measured diffraction efficiency for the *4 inch design* ZP. Shown are the diffraction efficiencies for the collimated order m=+1 beam (left) and the divergent order m=0 beam (right). The diffraction efficiencies are plotted two-dimensionally (top panels), depending on ZP radius (middle panels), and depending on ZP azimuth (bottom panels). The azimuthal orientation is indicated in by the dashed line in the top panels.

The results for the collimated beam, $I_{m=+1}/I^0$, are mapped in Fig. 13(a). The corresponding values are also shown as a function of ZP radius and ZP azimuth in Fig. 13(c). The results show that the intensity is maximum at a ZP radius of 10 mm and decreases to the edge and toward the ZP center.
The results for the direct beam, $I_{m=0}/I^0$, are mapped in Fig. 13(b). The corresponding values are also shown as a function of ZP radius and ZP azimuth in Fig. 13(d). The results show that the intensity is minimal at a ZP radius of 10 mm and increases to the edge and toward the ZP center. For ZP radii larger 25 mm the intensity

increases strongly. This is expected, since the PI foil occupies a larger area than the structured area. This can be clearly seen in Fig. 11. This causes that the efficiency of the direct beam is not reduced at the expense of diffraction orders $m \neq 0$. In this range, the efficiency is reduced only by the thickness of the PI layer.

2.2 Characterization of the 6 inch ZPC

The X-ray performance of the *6 inch design* ZP is determined the same way as the performance of the *4 inch design* ZP. The results are plotted as a two-dimensional map and as function of ZP azimuth and ZP radius. An essential difference of the *6 inch design* ZP is that the ZP geometry does not coincide with the wafer geometry. As seen in Fig. 14, this is not possible because the optic is designed as a ZP segment. Since the fabrication process is symmetrical to the wafer geometry, the parameters of efficiency and angular resolution are also shown dependent on the wafer azimuth and on the wafer radius.

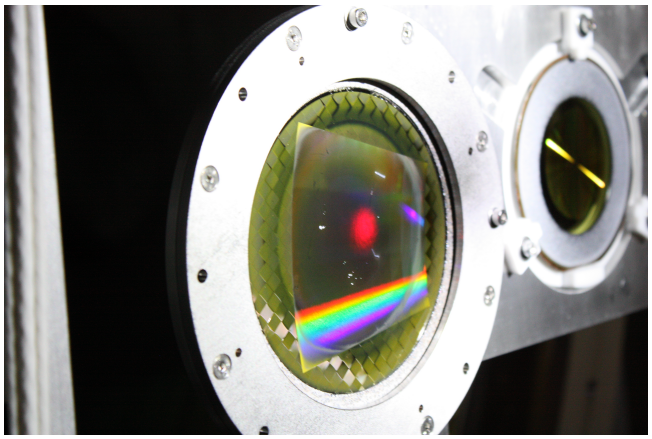

Figure 14: The *6 inch design* phase ZP mounted in the PANTER X-ray test facility. The segmented ZP has an inner radius of 12.5 cm and an outer radius of 20 cm. The phase shift, optimized for an energy of 1.49 keV, the Al-K$_\alpha$ emission line, is realized by a tungsten structure with a height of 435 nm.

Because of the low diffraction efficiency two different pin-hole masks were used. To determine the efficiency a rough mask with large diameter pin-holes was used. To determine the angular resolution, a fine mask with small diameter pin-holes was used. Thus, the efficiency can be determined analogous to the *4 inch design* ZP in equidistant bins. Because of the long exposure time required for the test, the analysis has been limited to a 40% of the ZP.

2.2.1 Angular resolution

The results obtained for the angular resolution are shown in Fig. 15. Fig. 15 shows the angular resolution depending on ZP geometry and wafer geometry. The top panel of Fig. 15 shows the measured divergence angle α_{div} and the measured collimation angle α_{col} depending on the ZP radius. The measured angles are in agreement with the divergence of a source at a distance of 131.8 m, which is over-plotted with the dashed blue line.
The second and third panel show the collimation quality measured by the difference of $\Delta\alpha = \alpha_{col} - \alpha_{div}$ depending on ZP radius and ZP azimuth respectively. The bottom panel shows the collimation quality depending on the wafer azimuth. On average, the values of $\Delta\alpha$ are (-0.01 ± 0.29) arc sec.
Looking at the second plot in more detail, an increase of $\Delta\alpha$ depending on the ZP radius can be identified. This trend can be modeled by a linear fit, which is over-plotted with the dashed black line. The result of the linear fit, having a $\chi^2_{red} = 1.02$, is $\Delta\alpha = -1.62\,\text{arc sec} + 0.0096\,\text{arc sec}\,\text{mm}^{-1}$. Hence, a systematic aberration effect can be claimed due probably to a radial distortion of the ZP.
The third and fourth plot in Fig. 15 shows that the effect is not only dependent on the ZP radius, but also depends on the ZP and wafer azimuth. For a better overview different ZP radii sections are color-coded. $\Delta\alpha$ is maximal at the mean ZP azimuth of 97.5° and drops to the borders at 85° and 110°. Depending on the wafer geometry, $\Delta\alpha$ has a maximum at 90° and a minimum at 180°.
The results obtained so far indicate that a distortion is present in the ZP. From the design of the ZP follows that this distortion must be caused by the PI layer, as PI is the support structure and tungsten is embedded. This seems all the more plausible, because even during the first manufacturing experiments a distortion of the PI

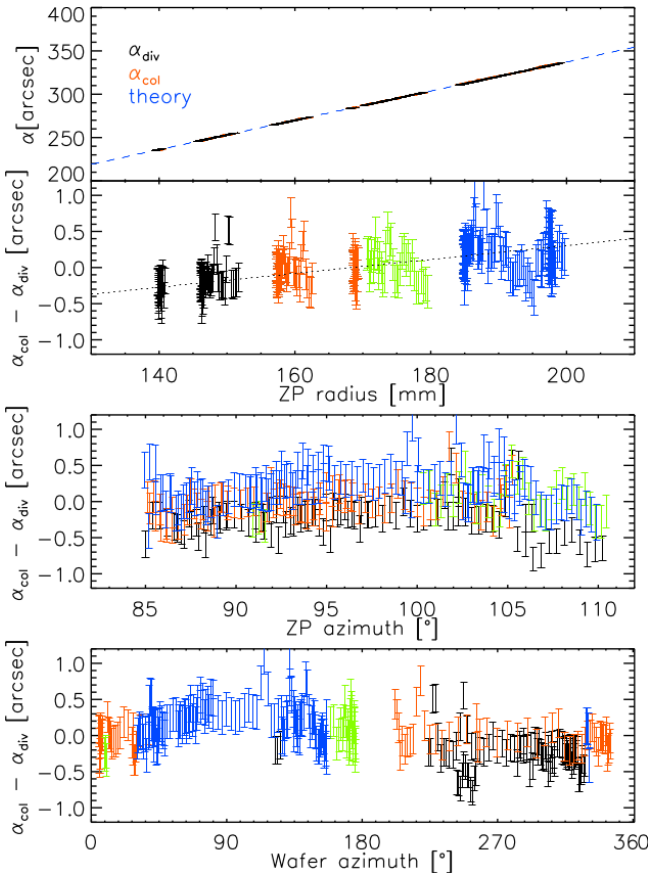

Figure 15: The results obtained for the angular resolution. The top panel shows the measured divergence angle α_{div} and the measured collimation angle α_{col} depending on the ZP radius. The panel below shows the collimation quality measured by the difference of $\Delta\alpha = \alpha_{col} - \alpha_{div}$ depending on ZP radius. For a better overview different ZP radii sections are color-coded. The third panel shows the collimation quality measured by the difference of $\Delta\alpha = \alpha_{col} - \alpha_{div}$ depending on ZP azimuth that is along the curvature of the ZP itself. The bottom panel shows the collimation quality depending on the wafer azimuth. The wafer azimuth is given by the circle that circumscribes the ZPC.

layer was observed. In a first successful approach, this distortion was reduced by the fact that tungsten squares outside the ZP structured area remain. These tungsten squares are clearly visible in Fig. 14. In principle, two causes of shrinkage can be identified: firstly, the PI used is cured at 200 °C; secondly PI out-gases in vacuum. A more extensive study and test are necessary to explain in a more exhaustive way the distortion.
In summary, the ZP collimated beam has an divergence consistent with zero of (-0.01 ± 0.29) arc sec, where the error is the statistical fluctuation of the values. Considering the linear trend it can be claimed that the ZP segment has a systematic error. This linear trend causes a systematic error of ±0.4 arc sec. Compared to the resolution of the ATHENA Silicon Pores Optics (SPO) the angular resolution of the ZP is better by a factor of ten. ZP aberrations in the angular resolution are therefore negligible compared to the aberrations in the angular resolution of ATHENA SPO. Thus, this ZP can be used as a collimator to measure the angular resolution of e.g. SPO.

2.2.2 Efficiency

A second data set was taken to determine the diffraction efficiency for the *6 inch design* ZP. This data set, shown in Fig. 16, measures the ZP efficiency in equidistant areas, due to the coarser grid and larger size pinhole diameters. Fig. 16(b) illustrates clearly how in the area of ZP segment the efficiency of diffraction order $m = 0$ is reduced compared to the surrounding non-structured PI film. Due to the design [1] the highest efficiency is expected for diffraction orders $m = \pm 1$ and the intensity of the zero diffraction order is reduced at the expense of higher diffraction orders.
This leads to the values, which are shown in Fig. 17. Analogous to Sect. 2.1.2 the efficiency is mapped two-dimensional. The efficiencies for the diffraction order $m = 1$ are shown in Fig. 17(a) and for $m = 0$ in Fig. 17(b).

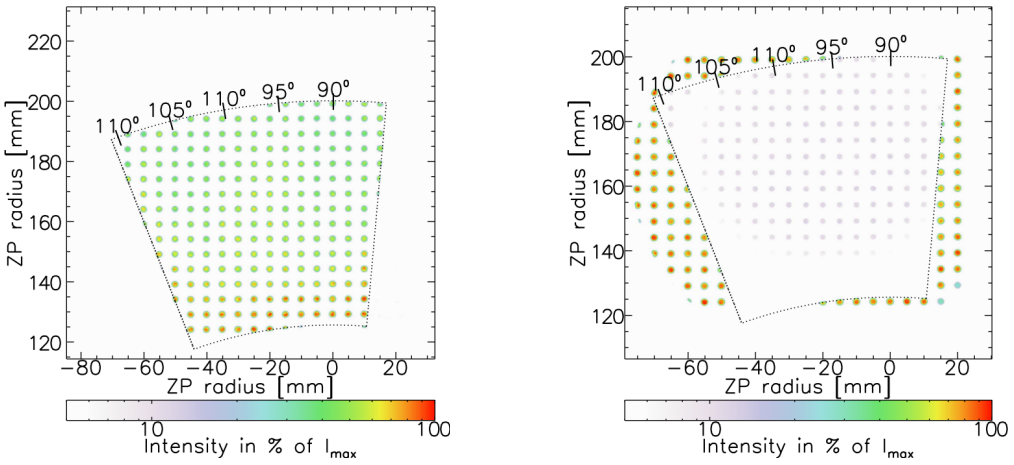

(a) Diffraction order $m = +1$.

(b) Diffraction order $m = 0$.

Figure 16: Two-dimensional intensity image of the measurement to determine the diffraction efficiency. The segment boundaries are indicated by the dotted lines.

The segment and wafer boundaries are indicated by a dotted and a dashed line, respectively. In addition, the efficiencies are shown in polar coordinates. Since for the *6 inch design* ZP the segment geometry does not match the wafer geometry, the diffraction efficiency is plotted in two polar coordinate systems: The polar coordinates defined by the segment geometry (ZP radius and ZP azimuth) with origin in the ZP center and the polar coordinate system defined by the wafer geometry (wafer radius r_{wafer} and wafer azimuth) with origin in the wafer center. The coordinate systems are defined in Fig. 17(a) and Fig. 17(b). The efficiencies for the diffraction order $m = +1$ are plotted in Fig. 17(c) and for $m = 0$ in Fig. 17(d).
The plots show multiple effects, which are interpreted below. Firstly, the two-dimensional plots show a radial structure relative to the wafer geometry. This is also evident in the radial plot depending on wafer geometry. In addition, a radial effect relative to the ZP geometry can be identified. This can be clearly seen in the corresponding plot panels of Fig. 17.
The measurements confirm that the collimated beam has the size of the ZP segment. Further the measurement set-up benefits if the collimated beam is flat. This means that the collimated beam is not shaded and homogeneous. In the *6 inch design* ZP shadows are avoided as the ZPC is realized on a carrier film of PI and does not need any support grid. The measurements confirm that the collimated beam is not shaded, however, the collimated beam is inhomogeneous. These inhomogeneities cannot be corrected by the experimental set-up. However, the inhomogeneities are mapped and this map can be used to compare measured PSF of a mirror with simulated PSF employing ray tracing. Hence, a ZPC with a nearly flat collimated beam in size greater than 65 mm × 75 mm has been realized. This is ideally suited to measure ATHENA type SPO.

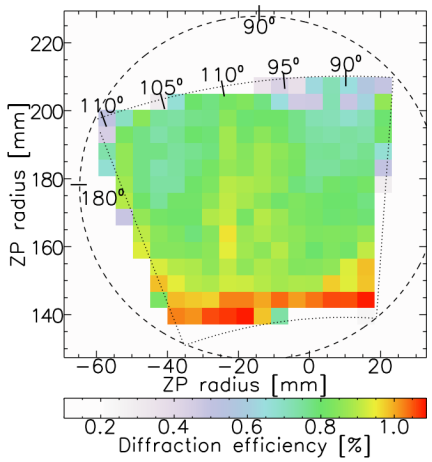

(a) Diffraction order m = +1: Two-dimensional map.

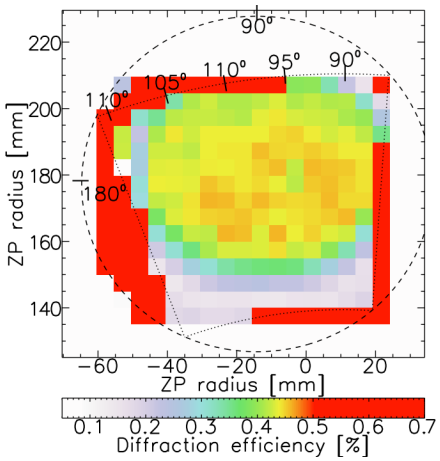

(b) Diffraction order m = 0: Two-dimensional map.

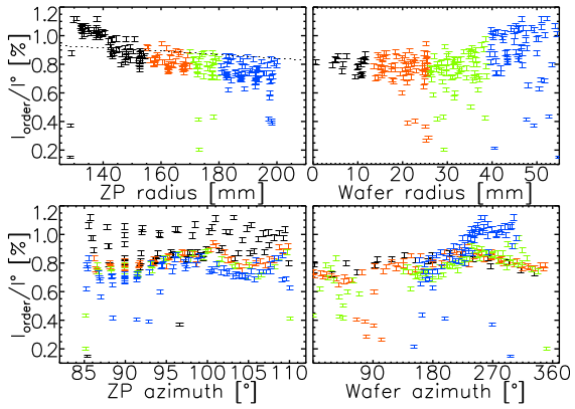

(c) Diffraction order m = +1: Radial (top) and azimuthal (bottom) diffraction efficiency depending on ZP (left) and wafer (right) geometry.

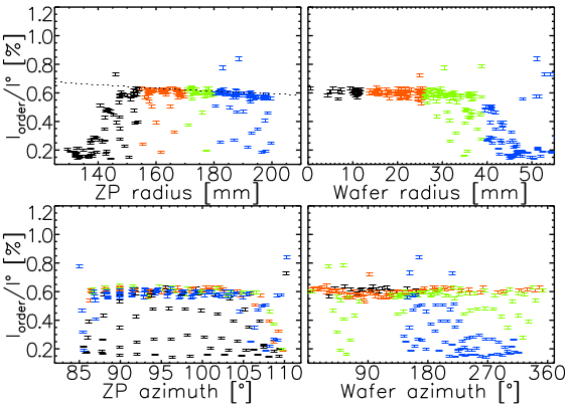

(d) Diffraction order m = 0: Radial (top) and azimuthal (bottom) diffraction efficiency depending on ZP (left) and wafer (right) geometry.

Figure 17: The measured diffraction efficiency for the *6 inch design* ZP. The diffraction efficiencies for the collimated beam (order m=+1) are shown in sub-figures ((a)) and ((c)). The diffraction efficiencies for divergent beam (order m=0) are shown in sub-figures ((b)) and ((d)). The diffraction efficiencies plotted two-dimensional (top panels), depending on radial geometry (middle panels), and depending on azimuthal geometry (bottom panels). Sub-figures ((c)) and ((d)): The diffracted beam is plotted depending on ZP geometry (left) and wafer geometry (right). In sub-figures ((a)) and ((c)) the ZP geometry and wafer geometry is indicated by the dotted and dashed lines respectively.

3 Characterizing Wolter optics with a ZPC

In this section we demonstrate a ZP can be used as a collimator for the PANTER X-ray test facility. We report the results obtained during two test campaigns dedicated to the measurements of optics with focal length of 24 and 1.6 meters.
The ZPC is located at a distance of 122 m from to the X-ray source. According to the ZP design the first order diffracted X-ray beam is parallel. This diffracted beam is then focused by a Wolter type X-ray optic (figures 4 and 1).
A critical issue when using a ZP as collimator is the overlap caused by higher diffraction orders.
Two ZP has been used one with small (4 inch design) and one with a bigger radius (6 inch design). The *6 inch design* ZPC it is shown that the overlapping between adjacent orders can be reduced to a negligible level. In conclusion Thus the *6 inch design* ZPC can be used to characterize a Wolter type optic with a collimated X-ray beam at the PANTER X-ray test facility.

3.1 The 4 inch ZPC demonstrator used with a SPO with nominal f=20 m

The 4 inch ZPC has been used to demonstrate the feasibility of a parallel beam (As reported in section 2). The same ZPC has been used with the XOU-0019 with a nominal focal length f_{Mirror} = 20 m. The setup is reported in fig. 5.
In the big chamber of the PANTER facility and without ZPC beam it is possible to measure optics with a nominal focal length smaller than 9 meters. In order to measure optics with higher focal length a chamber extension has been designed and it is possible to measure optics (without ZPC) up to 20 meters focal length. With a ZPC will be possible, upon some hardware modification, to measure a optics with a focal length of 12 meters (up to a maximum of 20.3 meters). At the time the test were performed, only the SPO with a nominal focal length of 20 meters was available. According to the thin lens equation the SPO has at PANTER an image distance of $b_{m=0}$ = 24 m due to the finite source distance of g = 123 m.
This optics was used to prove that (figure 18):

- the order are overlapping each other creating a sort of background noise, or a overlapping image.
- increasing the radius of the ZPC the separation of the order increase. This result carries to the design of the 6 inch ZPC.

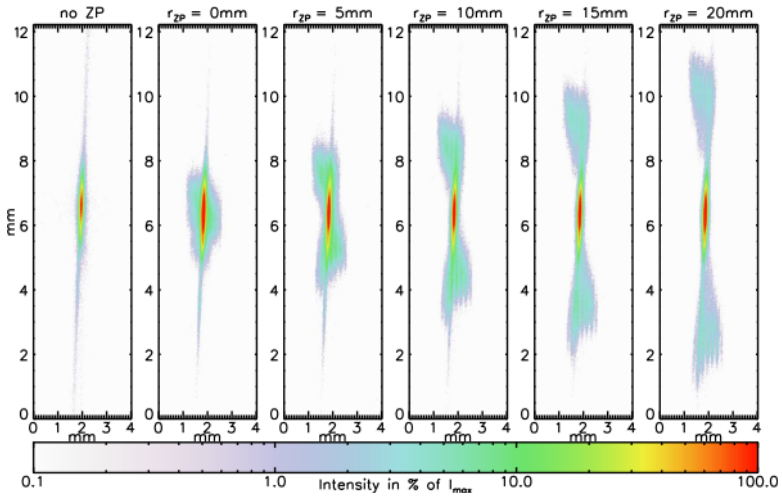

Figure 18: With increasing ZP radius the background can be reduced. SPO point images are measured at the zero order nominal image distance $b_{m=0}$ = 24 m. On the left is shown the point image of the SPO without the ZPC. The other images show measurements when installing the ZPC. The in focus point image of the direct beam is superimposed with the out-of-focus contributions mainly due to the first diffraction orders. With increasing ZP radius r_{ZP}, the in focus and out focus contributions due to the different orders can be separated in the detector plane. For the maximal ZP radius r_{ZP} = 20 mm the in focus point image of the direct beam (order m = 0) is comparable to the image without ZP.

As already mentioned, the ZPC was mounted in a distance of 122 m with respect to the X-ray source. Hence, for order m = +1 the X-ray beam is collimated. Illuminating the SPO with the ZPC influences the point image in

the way, that for each grating order m a spot exists in the detector planes. Figure 18 shows how it is possible to separate the order in the detector plane increasing the radius of the ZP.
In Fig. 18 on the left is shown the point image of the masked SPO without the ZPC. Placing the ZPC in the beam path influences the measurement in that the in focus point image of the direct beam is superposed with out of focus contributions mainly due to the first diffraction orders. For the three diffraction orders the images in Fig. 18 show the in focus contribution of the direct beam ($m = 0$), the extra focal contribution of the collimated beam ($m = +1$), and the the intra focal contribution of the divergent beam ($m = -1$). Different ZP radius r_{ZP} have been selected using the 5 mm × 5 mm aperture mask. With increasing r_{ZP} (from left to right in Fig. 18), the in focus and the out of focus contribution due to the different diffraction orders can be gradually better separated in the detector plane. For the maximal ZP radius $r_{ZP} = 20$ mm of the *4 inch design* ZPC (the right panel in Fig. 18) the in focus point image of the direct beam (order $m = 0$) is comparable to the image without ZPC, as the out of focus contributions of the collimated diffraction order $m = +1$ above and the divergent diffraction order $m = -1$ below the focused point image are far enough away in the detector plane.
In conclusion, using an outer region of the ZPC the disturbing overlapping caused by higher diffraction orders can be reduced. Therefore, the larger *6 inch design* ZP was realized as a segment ad tested with a shorter focal length optics.

3.2 Test campaign with the 6 inch design ZPC using a f=1.6 m optic

In this section we report the result of the use of a large radius ZPC (6 inch ZPC):

- With a bigger radius compared to the 4 inch ZPC the beam diffracted from different orders can be separated (Figure 20).
- The parallel beam permits to measure the nominal focal length of the optics without applying any mathematical correction, i.e.thin lens equation. See figure 21.

3.2.1 PSF image with and without ZPC

During the calibration of the eROSITA flight mirror assembly FM1 it has been possible to characterize parts of it using the *6 inch design* ZPC. The set-up along the optical axis z is shown in Fig. 1. In order to illuminate a SPO like segment of the eROSITA mirror a part of the mirror was selected using an aperture mask (Figure 2(a)). The area of the mirror, which was selected with the movable aperture mask for the here presented measurements, is indicated in blue. Fig. 2(b) shows a photo of the *6 inch design* ZPC. The exit aperture, a square with edge length 36 mm, was used to get a collimated beam size similar to the stack height of a SPO mirror module. The segment of the eROSITA mirror has been first measured without the ZPC. Fig. 19 shows the focused point image measured with the eROSITA type X-ray detector eROSITA qualification model (eROqm).

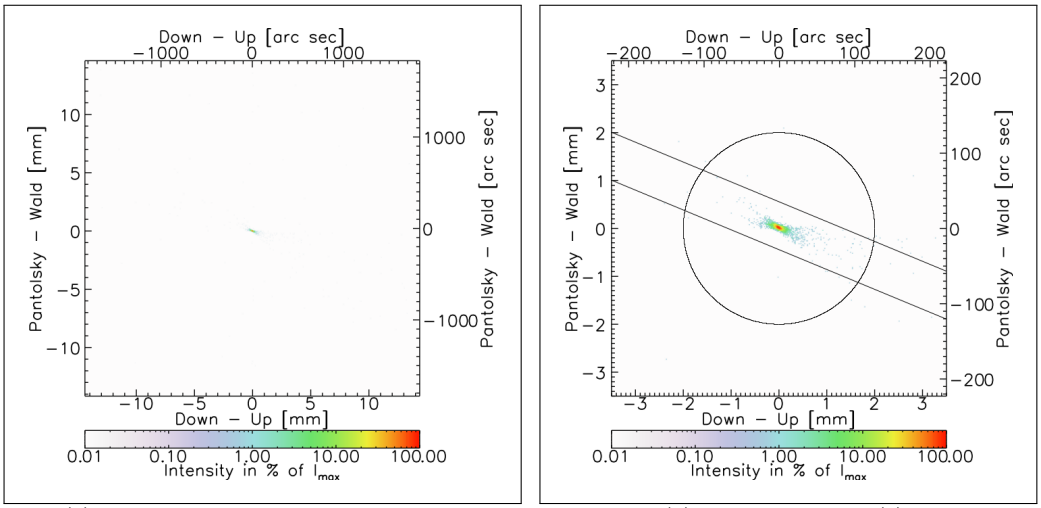

(a) Point image measured with eROqm

(b) Zoom of figure 19(a)

Figure 19: Measurement without ZPC

Then the same measurement were repeated with the ZPC. The image are reported in figure 20. Important here is that the PSF of the mirror can be measured and that the overlapping caused by the ZPC higher diffraction orders, is small and does not influence the measurement results. Figure 20 shows two additional point images. An extra focal point image by the collimated beam of order $m = +1$ (right) and an intra focal point image of order $m = -1$ (left). The diagonal shadow in the out-of-focus point images is due to the support spider the eROSITA mirror.

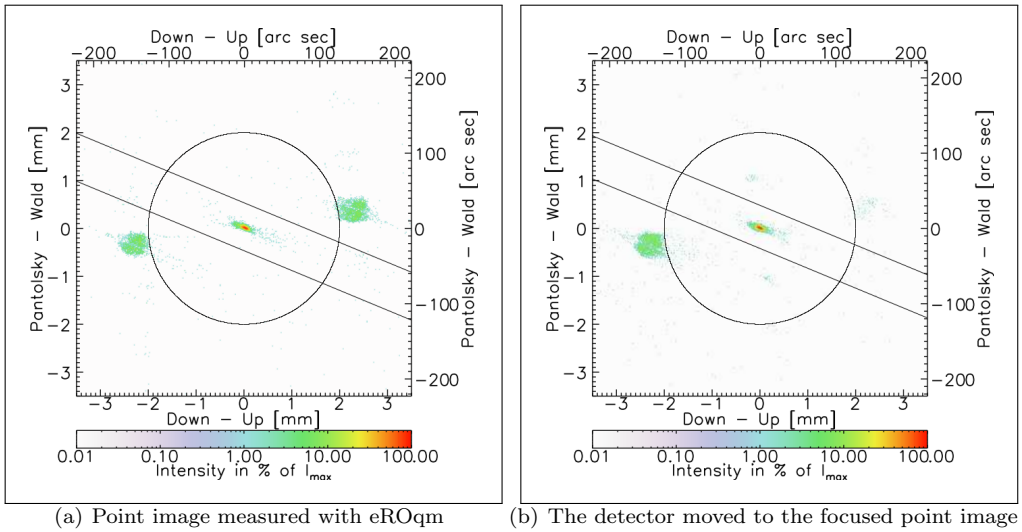

(a) Point image measured with eROqm

(b) The detector moved to the focused point image of order $m = +1$. The point image of beam order $m = 0$ is extra focal.

Figure 20: Measurement with ZPC. Two additional point images are detected. An extra focal point image by the collimated beam of order $m = +1$ (right) and an intra focal point image of order $m = -1$ (left).

3.2.2 Focal distance with and without ZPC

One major difference when measuring the X-ray optics with a divergent beam instead of a collimated beam is the image distance i. According to the thin lens equation the image distance s of the focused point image depends on the object distance s (in our case it is represented by the the source).
Due to the finite source distance at PANTER the image distance of the divergent zero order beam is $b_{m=0} = 1622.7\,\text{mm}$ while the image distance for the collimated beam of order $m = +1$ equals the mirror focal length $b_{m=+1} = f = 1601.8\,\text{mm}$.
The image distance is determined by measuring the focused point image along the optical axis z. By analyzing these measurements the Half Energy Width (HEW) of the mirror can be calculated for the diffraction orders $m = +1$ and $m = 0$ depending on the optical axis z position. The results are plotted in Fig. 21.
Color coded are the HEW values of diffraction orders $m = +1$ (red) and $m = 0$ (black). In order to measure the image distance the minimal HEW has to be determined. Close to the proper image distance the HEW values depending on optical axis position z can be approximated by a hyperbola. The corresponding hyperbola fits are over-plotted in blue in Fig. 21. By determining the vertex of the hyperbola fit the minimal HEW and consequently the corresponding optical axis position z is determined. The resulting vertex values are summarized in Table 2.
Based on the graph reported in figure 21, the difference between the image distance of the collimated beam order $m = +1$ and the image distance of the divergent beam order $m = 0$ is calculated to be $\Delta_{Measure} = (21.0 \pm 0.2)\,\text{mm}$. This distance value can be compared to the theoretical calculated difference in image distance of $\Delta_{theory} = (20.99 \pm 0.02)\,\text{mm}$. Both values fit together within the given errors.
The theoretical image distance value is derived by the assumption that the thin lens equation is applicable for a Wolter optic and the X-ray measurements are in agreement with the previous mentioned assumption..
As a further result the HEW values of the focused point images are determined. By illuminating the mirror with the divergent beam of order $m = 0$ and with the collimated beam of order $m = +1$ similar HEW values of (15.0 ± 0.5) arc sec and (15.00 ± 0.50) arc sec respectively are measured giving two value that are perfectly comparable.

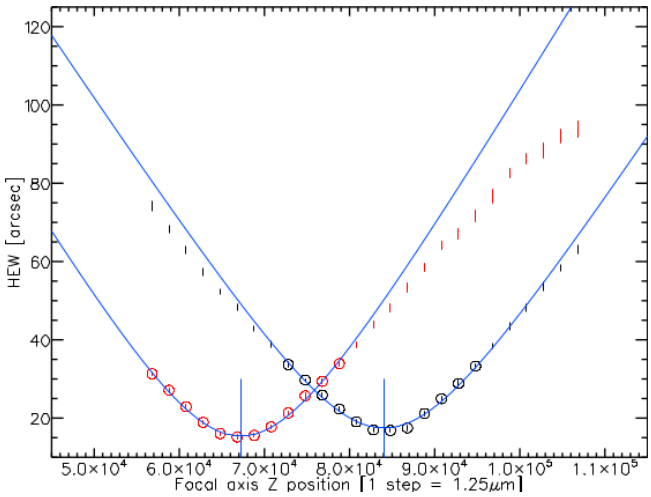

Figure 21: Measured HEW values depending on optical axis position z to determine the image distance. Color coded are the HEW values of diffraction order $m = +1$ (red) and $m = 0$ (black). In order to measure the image distance the minimal HEW has to be determined. Close to the proper image distance the HEW values depending on optical axis position z can be approximated by a hyperbola. The hyperbola fits, over-plotted in blue, are based on the HEW values over-plotted with circles.

Table 2: Measured focal length values.

Measure	Value
Measured position for order $m = +1$	$z = 67\,197 \pm 88$ Steps[a]
Measured position for order $m = 0$	$z = 84\,022 \pm 162$ Steps
Measured delta focal length	$\Delta_{Measure} = (21.03 \pm 0.23)$ mm
Calculated focal length	$f = (1601.778 \pm 0.501)$ mm
Measured image distance	$b_{m=0} = (1622.700 \pm 0.051)$ mm[b]
Calculated delta focal length	$\Delta_{theory} = (20.992 \pm 0.020)$ mm

[a] 1 Step = 1.25 µm
[b] $g = (123.822 \pm 0.100)$ m

4 Conclusions

At the PANTER X-ray test facility different setups are available to measure the master XOU:

- Setup without ZPC:
  - this setup are affected by the finite size of the source that give contribution to the resolution of about 1 arcsec;
  - beam is divergent and the effective focal length of the optics has to corrected by two factors: thin lens equation and off axis measurement [6].
- Setup with ZPC. With the test described in this document we can conclude that the ZPC can be used to characterize a Wolter type Optics:
  - the ZPC produces a parallel beam with an angular divergence smaller than 0.5 arcsec i.e. 10 times better than the expected angular resolution of the master SPO optics;
  - the diffracted beam is not affected by the dimension or shape of the PANTER X-ray source;
  - the focal length measured with ZPC is the same that will be measured with the X-ray source at infinity;
  - the contribution to the noise of the higher diffraction order can be reduced increasing the radius of the ZPC and restrict the analysis on the detector to the region of interest.

– The PSF measured with the Zone Plate collimated beam of order m = +1 and the PSF measured without the ZPC have equal HEW values. It follows that the ZP does not cause significant angular aberrations collimating the beam.

With some mechanical modification of the big chamber setup it will be possible to test the SPO optics with a focal length of 12 meters directly in the big chamber without using the extension chamber. The mechanical modification have been evaluated and are under implementation. A setup has been designed (Figure 8 at page 8). This solution has two main advantages:

1. it reduces the installation time
2. it permits to use the Third Roentgen Photon Imaging Camera (TRoPIC) detector. In fact, in the extension chamber we can only use the PIXI detector that is not energy sensitive.

At present time, the PANTER X-ray facility is ready to measure optics with 5 arcsec resolution.

References

[1] C. Pelliciari, B. Menz, *et al.*, "Design report on the collimated X-ray beam," Tech. Rep. Deliverable D8.3 - D37, Dec. 2016.

[2] C. Pelliciari, "Implementation of the improved parallel X-ray beam for testing high resolution optics," Tech. Rep. AHEAD-WP8-D8.7-D41-ZPC, Apr. 2018.

[3] B. J. Menz. PhD thesis.

[4] B. Salmaso, D. Spiga, S. Basso, *et al.*, "Progress in the realization of the beam expander testing x-ray facility (BEaTriX) for testing ATHENA's SPO modules," *SPIE* **10699**, 2018.

[5] C. Pelliciari, D. Spiga, *et al.*, "BEaTriX, expanded X-ray beam facility for testing modular elements of telescope optics: an update ," *Proc. SPIE* **9603**(56), 2015.

[6] C. Pelliciari, "Report of the measurements of the different X-ray optics units compared with the simulations," Tech. Rep. Deliverable D8.8 - D42, Jan. 2019.

[7] C. Pelliciari, "Characterization of master high resolution XOU for test performed at PANTER facility.," Tech. Rep. Deliverable D8.5 - D39, May 2018.